Gold Photochemistry

DOI: 10.1002/ange.201308135

Approaching White-Light Emission from a Phosphorescent Trinuclear Gold(I) Cluster by Modulating Its Aggregation Behavior**

*Wen-Xiu Ni, Mian Li, Ji Zheng, Shun-Ze Zhan, Yu-Min Qiu, Seik Weng Ng, and Dan Li**

The development of white-light-emitting materials and devices[1] plays an important role in the next-generation solid-state lighting technology.[2] In this field, there are generally two types of working principles to achieve white light, either from multiple cooperating emitters,[3] or from a single multifunctioning emitter.[4] Both cases generate at least dual emissions (e.g. bluish green and reddish orange) that are complementary colors of white light. The single multifunctioning emitter type is superior to the multiple cooperating emitters because it can prevent phase-separation and color variation problems.[1] However it remains a challenge to design and synthesize single molecules, especially phosphorescent coordination complexes, that emit across the broad visible spectrum and exhibit white light.[5]

Some significant progress has been made for luminescent Pt^{II} complexes by the groups of Che[6] and Yam,[7] who took advantage of the monomer–excimer equilibrium that facilitates the broad band emissions in these systems. Such in-depth studies have warranted the application of Pt^{II} complexes in single-dopant white organic light-emitting devices (WOLEDs), advanced also by these two groups[8] and others.[9] Based on the working principle of Pt^{II} complexes, two structural prerequisites have to be fulfilled to generate white light from dual emission bands: 1) there should be a certain functional group acting as a chromophore to ensure the luminescent efficiency of the monomer; 2) the designed molecule requires a structure with little steric hindrance (e.g. the square-planar configuration of Pt^{II} complexes[6,7]) to facilitate the formation of the excimer when the monomers are positioned in close proximity to each other. Gold complexes have shown promise in OLED developments, not only because they present rich photochemistry, but also because they have low-toxicity and are environmentally benign.[10] However, unlike the Pt^{II} complexes, which are widely investigated, the potential for WOLEDs based on photoluminescent Au^{I} complexes has been much less evaluated.

In an attempt to synthesize gold white-light emitting materials, we focus on a family of trinuclear d^{10} M^{I} pyrazolate clusters (M = Cu, Ag, Au) that have been of interest to us[11] and others.[12] Among these, the Au^{I} analogues have potentially useful properties: they have a strong tendency to form excimers linked by $Au^{I}\cdots Au^{I}$ bonding (aurophilicity[13]), which is supported by their rigid planar configuration and linear coordination mode, and give bright and long-lived phosphorescence.[10] The excimers of trinuclear Au^{I} pyrazolate complexes,[12,14] regulated by self-aggregation, usually emit in the low-energy (LE) orange–red region. However, the generation of white light requires the cooperation of the high-energy (HE) blue–green region of the monomer, which is usually absent in reported M^{I} pyrazolate clusters.[11,12] Herein the thiophene group, which can increase light absorption to promote luminescence,[15] is introduced as a substituent on pyrazole, to enhance the high-energy emission of the monomer.

The absorption spectrum of the selected ligand, 3-(2-thienyl)pyrazole (H**L**), exhibits two absorption peaks at 273 and 289 nm (intraligand $^1\pi$–π^* transition) and shows blue–green emission ($\lambda_{em} = 330$ nm) in CH_2Cl_2 solution.[15a] The trinuclear [{Au(**L**)}$_3$] cluster (Figure 1, left) is prepared in a high yield by treating [Au(tht)Cl] (tht = tetrahydrothiophene) with H**L**. The product is characterized by IR, UV/Vis spectra, ^{1}H NMR spectroscopy, elemental analysis (C, H, N), MALDI-TOF mass spectrometry and X-ray crystallography (see Supporting Information and Ref. [18] for details). The absorption spectrum of [{Au(**L**)}$_3$] in CH_2Cl_2 displays two peaks at 256 and 290 nm (Figure S1 in the Supporting Information), similar to that of H**L**. As expected, the high-energy band ($\lambda_{em} = 408$ nm) of the [{Au(**L**)}$_3$] monomer occurs upon the excitation at 340 nm in aerated CH_2Cl_2 solution (Figure S6). The red shift of the high-energy band compared with that of H**L** is attributed to metal-coordination-related charge transfer. A broad shoulder covering 500–600 nm is also observed. This featureless low-energy band originates from the triplet excimer formed from the chair stacking (Figure 1, right) of the [{Au(**L**)}$_3$] monomers that are regulated by $Au^{I}\cdots Au^{I}$ bonding (aurophilic interactions).[12–14]

[*] Dr. W.-X. Ni, M. Li, J. Zheng, Dr. S.-Z. Zhan, Y.-M. Qiu, Prof. Dr. D. Li
Department of Chemistry and Research Institute for Biomedical and Advanced Materials, Shantou University
Guangdong 515063 (P. R. China)
E-mail: dli@stu.edu.cn
Prof. Dr. S. W. Ng
Department of Chemistry, University of Malaya
50603 Kuala Lumpur (Malaysia)
and
Chemistry Department, Faculty of Science
King Abdulaziz University
PO Box 80203 Jeddah (Saudi Arabia)

[**] The work was supported by 973 Program (Nos. 2013CB834803 and 2012CB821706), the National Natural Science Foundation for Distinguished Young Scholars of China (No. 20825102), and the National Natural Science Foundation of China (Nos. 21171114 and 91222202). W.-X.N. thanks the funding of China Postdoctoral Science Foundation (No. 2012M521622) and Guangdong Natural Science Foundation (No. S2012040006968). S.W.N. thanks the funding of the Ministry of Higher Education of Malaysia (Grant No. UM.C/HIR-MOHE/SC/03). We thank Prof. Tai-Chu Lau of the City University of Hong Kong for help on physical measurements.
Supporting information for this article is available on the WWW under http://dx.doi.org/10.1002/anie.201308135.

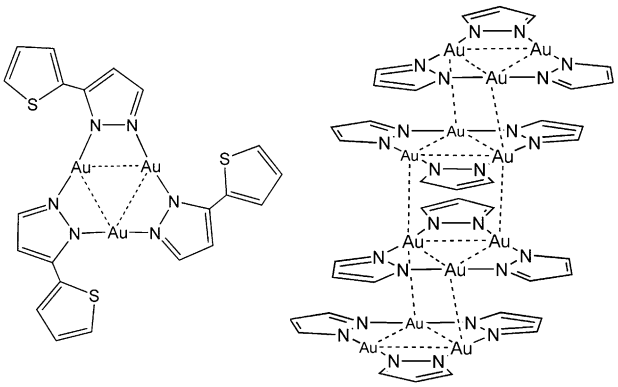

Figure 1. Structural formula of the [{Au(**L**)}$_3$] cluster (left) and its common chair-stacking pattern forming the excimer (right). Dashed lines indicate aurophilic interactions.

To demonstrate the monomer–excimer equilibrium which is strongly concentration dependent, we performed solution-state luminescence measurements. If the monomer–excimer equilibrium exists in this system, the relative intensity of the high-energy/low-energy bands will change upon variation of the concentration,[6–8] because in a more concentrated solution the possibility of excited [{Au(**L**)}$_3$] monomers meeting with ground-state monomers to form eximers will increase. Also the monomer–excimer equilibrium will be sensitive to external stimuli,[6–8] such as excitation energy and temperature variation, which will influence the number of excited-state monomers. In practice, when concentrated from 10^{-4} to 10^{-3} M, the emission color profiles (CIE-1931) of [{Au(**L**)}$_3$] in aerated CH_2Cl_2 solution shift towards the white-light region (Figure 2c), with the low-energy shoulder becoming more apparent in concentrated solution (Figure S6). This shift is consistent with the speculation that higher concentration facilitates the self-aggregation of the planar [{Au(**L**)}$_3$] cluster. The resulting triplet phosphorescent excimer responsible for the low-energy emission may be quenched by aerial oxygen. Therefore, after the degassing procedure, a second peak at 558 nm (decay lifetime 7.4 μs) emerges in the low-energy region (Figure 2a, $\lambda_{ex} = 340$ nm), confirming the excimeric triplet state. The slight red shift of the high-energy band from 402 to 408 nm upon increasing concentration is due to the interligand π–π stacking between the [{Au(**L**)}$_3$] clusters. At a concentration of 10^{-3} M, the spectrum exhibits a clear dual emission, with a CIE-1931 coordinate (0.28, 0.29) and a quantum yield of 0.259.

When the excitation energy changes to 370 nm, the relative intensity of the low-energy band is significantly enhanced (Figure 2b), thus improving the white-light quality (Figure 2c). Upon concentrated from 10^{-4} to 10^{-3} M, [{Au(**L**)}$_3$] exhibits higher degree of excimeric self-aggregation, which results in a clear red shift of the high-energy band to 450 nm (because of intermolecular π–π interaction), and the low-energy intensity surpasses that of high-energy band. At the concentration of 8×10^{-4} M, the intense dual emission band covering 400–700 nm has an optimal CIE-1931 white-light profile (0.31, 0.33) and a quantum yield of 0.413. The pure white light can be a combination of blue–green and orange–red emissions that are of competitive or even equal relative intensities, as observed in this case.

The proposed monomer–excimer equilibrium can give rise to white-light emission through the combination of the dual emissions from the [{Au(**L**)}$_3$] monomer and the excimer which is formed by aggregation in the solution state. However, the control of the aggregation behavior to give white light in the solid state is very difficult. Fortunately, we are able to crystallize two forms of [{Au(**L**)}$_3$], namely ***a*** and ***b*** (see Supporting Information for details), which exhibit orange–red and white emissions (Figure 3b), respectively, under UV lamp (365 nm) at room temperature. From the emission spectra ($\lambda_{ex} = 370$ nm, room temperature), both the high-energy (475 nm) and low-energy (620 nm) bands occur, but the low-energy band is predominant for form ***a***, while the high-energy band is predominant for ***b***.

Crystal structures of ***a*** and ***b*** reveal the crucial differences on the stacking patterns of [{Au(**L**)}$_3$] (Figure 3a, see also Figure S3 and S4) in relation to their diverse emissions. In ***a*** only the common chair pattern (stacking A in Figure 3a, red box) is found, while in ***b*** there coexist two patterns (stacking A + B with 1:1 ratio in Figure 3a, green box) with an additional dimer stacking B. The stacking B exhibits weaker intermolecular $Au^I \cdots Au^I$ contacts (stacking A: within the

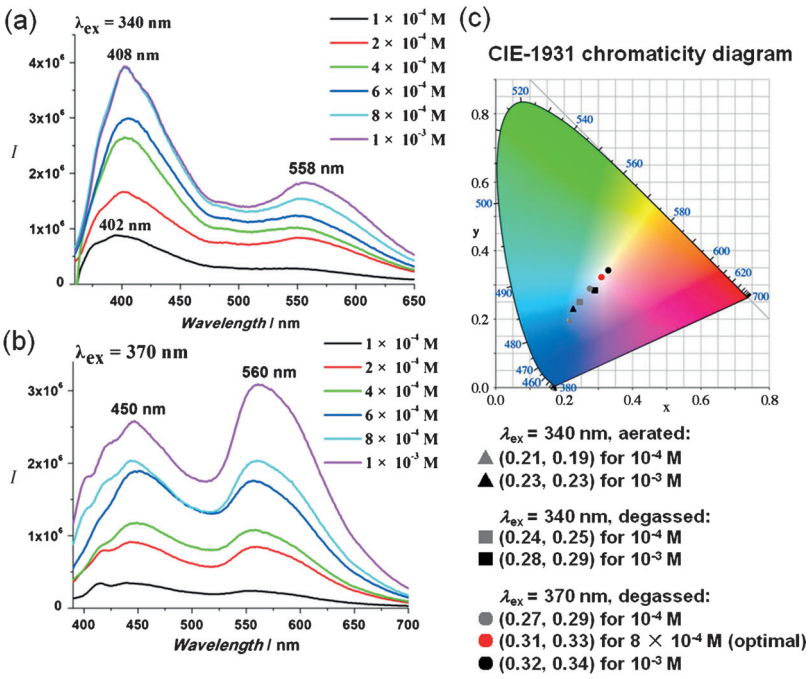

Figure 2. Emission spectra of [{Au(**L**)}$_3$] at various concentrations (in degassed CH_2Cl_2 solution at 298 K) upon the excitation at 340 nm (a) and 370 nm (b), and the corresponding emission color profiles in CIE-1931 (Commission Internationale d'Eclairage) chromaticity diagram (c). Note natural white light at (0.33, 0.33).

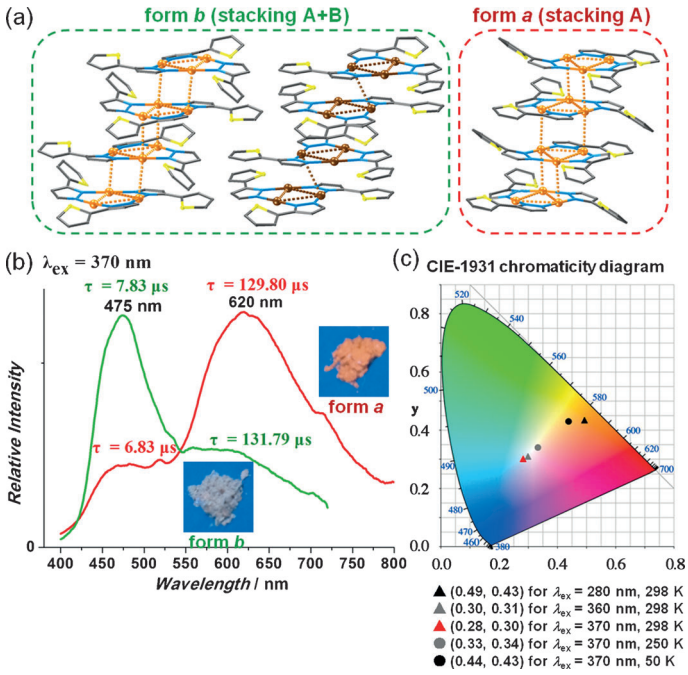

Figure 3. The two crystal forms ***a*** and ***b*** with their different stacking patterns (a). Their emission spectra at 298 K upon excitation of 370 nm (b). Inset: photographs of crystalline samples exposed to UV lamp. Emission color profiles of form ***b*** in CIE-1931 chromaticity diagram by varying excitation energy and temperature (c). See Table S2 for detailed intra- and intermolecular $Au^I\cdots Au^I$ distances.

range of 3.161–3.210 Å; stacking B: 3.380 Å at 298 K). All of the intermolecular $Au^I\cdots Au^I$ distances are significantly shorter than the sum of van der Waals radii of 3.6 Å, and also shorter than many reports of unsupported $Au^I\cdots Au^I$ bonds.[16] This dimer stacking pattern in ***b*** is unfavorable for excimer formation, and thus is responsible for the relatively lower intensity of low-energy band of ***b***, compared with that of ***a***. Another subtle structural difference that contributes to the relatively more intense high-energy band of ***b*** is the torsion angles between the thienyl and pyrazolate rings, with smaller values being found for those in stacking B of ***b*** (Figure 4, top). This enhanced conjugation effect resulting from the coplanarity of adjacent aromatic rings will promote the efficiency of the high-energy emission in stacking B, which is attributed to metal-mediated intraligand charge transfer (^{3}ILCT).

The above structural features are consistent with the uncommon white-light emission of form ***b***. We further optimized the CIE-1931 emission profile of this material by varying the excitation energy and temperature. As shown in Figure 3c, form ***b*** can exhibit near-white-light emission with CIE-1931 (0.30, 0.31) under 360 nm excitation and at room temperature (application working condition). The optimal white-light quality with CIE-1931 coordinate (0.33, 0.34) can be achieved at lower temperature (λ_{ex} = 370 nm, 250 K).

It is notable that upon varying excitation energy, the responses of the high-energy and low-energy bands of ***b*** differ clearly (Figure S7), indicating the excited state responsible for the high-energy band is different from the one that acts as the triplet acceptor[12] in the monomer–excimer equilibrium. In other words, the $[\{Au(\mathbf{L})\}_3]$ monomer can generate two excited states: a common one for forming the excimer that gives the low-energy band, and an uncommon one giving the high-energy band. Besides, the fact that higher energy excitation can prompt the lower energy band with microsecond lifetime (131.79 μs, 298 K) indicates the phosphorescent origin involves an intersystem crossing from a singlet ligand-to-metal-metal charge transfer (^{1}LMMCT) state to a triplet metal–metal (^{3}MM) emitting state proposed by Omary et al.[12] Furthermore, the splitting of the low-energy band under cryogenic conditions (Figure S8) directly validates the multiple ^{3}MM-states assumption for the excimers of trinuclear M^I pyrazolate clusters.[12b,c] The greater relative intensity of the low-energy band at low temperature is also related to the shorter intermolecular $Au^I\cdots Au^I$ distances in the structures at low temperature (see Table S2). This unsupported $Au^I\cdots Au^I$ bonding can also be enhanced by mechanical grinding, as evidenced by the increased intensity of the low-energy band after grinding (Figure S9).

To further interpret the origin of the monomer–excimer equilibrium in this system, we perform theoretical calculations to assess the role of the introduced thiophene group (see Supporting Information for computational details). Previous computational work has clarified which excimeric excited states of trinuclear M^I pyrazolate clusters are responsible for the low-energy emissions.[12c,d,17] In our system, the differences in the torsion angles between the thienyl and pyrazolate rings (Figure 4, top) and their influences on the molecular orbitals and excitation energy (Figure 4, bottom) are taken into

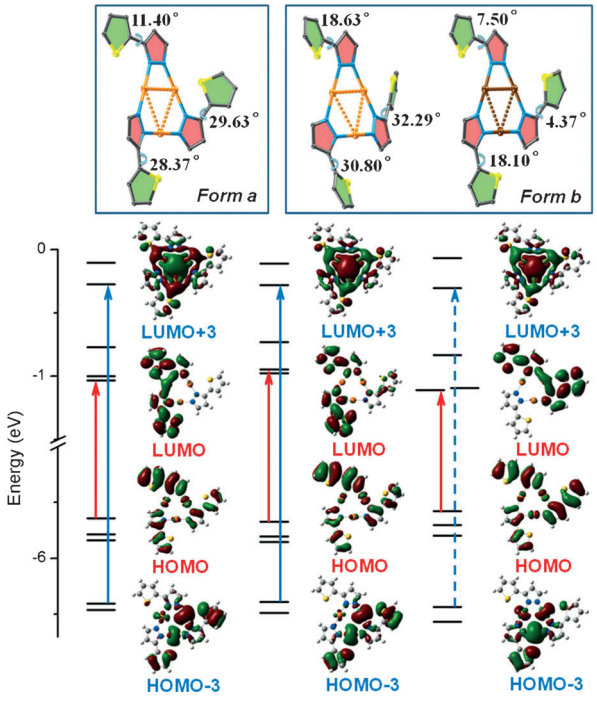

Figure 4. Torsion angles between the thienyl (green) and pyrazolate (pink) groups in the $[\{Au(\mathbf{L})\}_3]$ stacking of ***a*** and ***b*** (top) and their corresponding frontier molecular orbitals (bottom) marked with the main HOMOs→LUMOs transitions related to the excitation for high-energy (red arrows) and low-energy emission (blue arrows; dashed line: $f < 0.10$).

consideration. Two major clues can be extracted from the ground-state frontier molecular orbitals of different twisted conformers in ***a*** and ***b***. 1) In the high-energy region, the presence of stacking B with significantly smaller torsion angles and higher degree of conjugation gives rise to a narrower HOMO–LUMO gap (4.47 eV for stacking B in ***b***; 4.61 eV for A in ***a***; 4.69 eV for A in ***b***) by simultaneously lowering the LUMO and raising the HOMO energy levels. It also facilitates a stronger high-energy band intersystem-crossing from the ^{1}ILCT transition for ***b*** (oscillator strengths $f = 0.35, 0.19, 0.19$ for B in ***b***; $f = 0.33, 0.18, 0.10$ for A in ***a***; $f = 0.20, 0.31$ for A in ***b***). 2) In the low-energy region, there are remarkable cluster-centered transitions (^{1}CC) and metal-to-ligand charge transfers (^{1}MLCT) for stacking A ($f = 0.20, 0.12$ for A in ***a***; $f = 0.16, 0.10$ for A in ***b***) that could prompt the excimer formation accounting for the low-energy ^{3}MM emission. But these transitions are trivial ($f < 0.10$) for stacking B in ***b***, and thus form ***b*** with equal A and B population has a significantly lower low-energy intensity compared with that of ***a***.

A new trinuclear Au^I pyrazolate cluster with the thiophene substituent has been synthesized. The introduction of an organic chromophore, the thiophene group, gives rise to an excited state which is responsible for the uncommon high-energy blue–green emission. Together with the low-energy orange–red band, which originates from the monomer–excimer equilibrium and exhibits aurophilic phosphorescence, the compound is able to give off white light in both solution and solid states. Most interestingly, two crystal forms of the same component are isolated, which exhibit orange–red and white emissions, respectively. This observation is rationalized by structural, spectral, and theoretical studies. Further study will focus on enhancing the function as a white-light emitting material by doping device fabrication, especially trying to increasing its white phosphorescence quantum efficiency and thermal stability.

Received: September 16, 2013
Published online: November 19, 2013

Keywords: aurophilicity · excited states · gold cluster · phosphorescence · white light emission

[1] a) B. W. D'Andrade, S. R. Forrest, *Adv. Mater.* **2004**, *16*, 1585; b) M. C. Gather, A. Köhnen, K. Meerholz, *Adv. Mater.* **2011**, *23*, 233; c) G. M. Farinola, R. Ragni, *Chem. Soc. Rev.* **2011**, *40*, 3467; d) R. D. Costa, E. Ortí, H. J. Bolink, F. Monti, G. Accorsi, N. Armaroli, *Angew. Chem.* **2012**, *124*, 8300; *Angew. Chem. Int. Ed.* **2012**, *51*, 8178.

[2] a) E. F. Schubert, J. K. Kim, *Science* **2005**, *308*, 1274; b) C. J. Humphreys, *MRS Bull.* **2008**, *33*, 459; c) F. So, K. Kido, P. Burrows, *MRS Bull.* **2008**, *33*, 663.

[3] a) P. Coppo, M. Duati, V. N. Kozhevnikov, J. W. Hofstraat, L. De Cola, *Angew. Chem.* **2005**, *117*, 1840; *Angew. Chem. Int. Ed.* **2005**, *44*, 1806; b) Y. Ner, J. G. Grote, J. A. Stuart, G. A. Stozing, *Angew. Chem.* **2009**, *121*, 5236; *Angew. Chem. Int. Ed.* **2009**, *48*, 5134; c) Z. Zhao, J. W. Y. Lam, B. Z. Tang, *Curr. Org. Chem.* **2010**, *14*, 2109.

[4] a) G. He, D. Guo, C. He, X. Zhang, X. Zhao, C. Duan, *Angew. Chem.* **2009**, *121*, 6248; *Angew. Chem. Int. Ed.* **2009**, *48*, 6132; b) H. J. Bolink, F. D. Angelis, E. Baranoff, C. Klein, S. Fantacci, E. Coronado, M. Sessolo, K. Kalyanasundaram, M. Grätzel, Md. K. Nazeeruddin, *Chem. Commun.* **2009**, 4672; c) K.-C. Tang, M.-J. Chang, T.-Y. Lin, H.-A. Pan, T.-C. Fang, K.-Y. Chen, W.-Y. Hung, Y.-H. Hsu, P.-T. Chou, *J. Am. Chem. Soc.* **2011**, *133*, 17738.

[5] a) M.-S. Wang, G.-C. Guo, W.-T. Chen, G. Xu, W.-W. Zhou, K.-J. Wu, J.-S. Huang, *Angew. Chem.* **2007**, *119*, 3983; *Angew. Chem. Int. Ed.* **2007**, *46*, 3909; b) M.-S. Wang, S.-P. Guo, Y. Li, L.-Z. Cai, J.-P. Zou, G. Xu, W.-W. Zhou, F.-K. Zheng, G.-C. Guo, *J. Am. Chem. Soc.* **2009**, *131*, 13572; c) J. He, M. Zeller, A. D. Hunter, Z. Xu, *J. Am. Chem. Soc.* **2012**, *134*, 1553; d) Y. Liu, M. Pan, Q.-Y. Yang, L. Fu, K. Li, S.-C. Wei, C.-Y. Su, *Chem. Mater.* **2012**, *24*, 1954.

[6] a) S.-W. Lai, C.-M. Che, *Top. Curr. Chem.* **2004**, *241*, 27; b) S. C. F. Kui, S. S.-Y. Chui, C. M. Che, N. Zhu, *J. Am. Chem. Soc.* **2006**, *128*, 8297; c) Y. Sun, K. Ye, H. Zhang, L. Zhao, B. Li, G. Yang, B. Yang, Y. Wang, S.-W. Lai, C.-M. Che, *Angew. Chem.* **2006**, *118*, 5738; *Angew. Chem. Int. Ed.* **2006**, *45*, 5610; d) W. Lu, Y. Chen, V. A. L. Roy, S. S.-Y. Chui, C. M. Che, *Angew. Chem.* **2009**, *121*, 7757; *Angew. Chem. Int. Ed.* **2009**, *48*, 7621; e) S. C. F. Kui, Y.-C. Law, G. S. M. Tong, W. Lu, M.-Y. Yuen, C.-M. Che, *Chem. Sci.* **2011**, *2*, 221.

[7] a) V. W.-W. Yam, *Acc. Chem. Res.* **2002**, *35*, 555; b) K. M.-C. Wong, V. W.-W. Yam, *Acc. Chem. Res.* **2011**, *44*, 424; c) V. W.-W. Yam, K. M.-C. Wong, N. Zhu, *J. Am. Chem. Soc.* **2002**, *124*, 6506; d) A. Y.-Y. Tam, K. M.-C. Wong, V. W.-W. Yam, *J. Am. Chem. Soc.* **2009**, *131*, 6253; e) C. Po, A. Y.-Y. Tam, K. M.-C. Wong, V. W.-W. Yam, *J. Am. Chem. Soc.* **2011**, *133*, 12136.

[8] a) B.-P. Yan, C. C. C. Cheung, S. C. F. Kui, H.-F. Xiang, V. A. L. Roy, S.-J. Xu, C.-M. Che, *Adv. Mater.* **2007**, *19*, 3599; b) S. C. F. Kui, P. K. Chow, G. S. M. Tong, S.-L. Lai, G. Cheng, C.-C. Kwok, K.-H. Low, M. Y. Ko, C.-M. Che, *Chem. Eur. J.* **2013**, *19*, 69; c) E. S.-H. Lam, D. P.-K. Tsang, W. H. Lam, A. Y.-Y. Tam, M.-Y. Chan, W.-T. Wong, V. W.-W. Yam, *Chem. Eur. J.* **2013**, *19*, 6385.

[9] a) E. L. Williams, K. Haavisto, J. Li, G. E. Jabbour, *Adv. Mater.* **2007**, *19*, 197; b) X. Yang, Z. Wang, S. Madakuni, J. Li, G. E. Jabbour, *Adv. Mater.* **2008**, *20*, 2405; c) J. Kalinowski, V. Fattori, M. Cocchi, J. A. G. Williams, *Coord. Chem. Rev.* **2011**, *255*, 2401; d) L. Murphy, P. Brulatti, V. Fattori, M. Cocchi, J. A. G. Williams, *Chem. Commun.* **2012**, *48*, 5817; e) T. Fleetham, J. Ecton, Z. Wang, N. Bakken, J. Li, *Adv. Mater.* **2013**, *25*, 2573.

[10] a) V. W.-W. Yam, E. C.-C. Cheng, *Top. Curr. Chem.* **2007**, *281*, 269; b) V. W.-W. Yam, E. C.-C. Cheng, *Chem. Soc. Rev.* **2008**, *37*, 1806; c) V. W.-W. Yam, K. M.-C. Wong, *Chem. Commun.* **2011**, *47*, 11579; d) M.-C. Tang, D. P.-K. Tsang, M. M.-Y. Chan, K. M.-C. Wong, V. W.-W. Yam, *Angew. Chem.* **2013**, *125*, 464; *Angew. Chem. Int. Ed.* **2013**, *52*, 446; e) V. K.-M. Au, K. M.-C. Wong, D. P.-K. Tsang, M.-Y. Chan, N. Zhu, V. W.-W. Yam, *J. Am. Chem. Soc.* **2010**, *132*, 14273.

[11] a) J. He, Y.-G. Yin, T. Wu, D. Li, X.-C. Huang, *Chem. Commun.* **2006**, 2845; b) G.-F. Gao, M. Li, S.-Z. Zhan, Z. Lv, G.-h. Chen, D. Li, *Chem. Eur. J.* **2011**, *17*, 4113; c) S.-Z. Zhan, M. Li, X.-P. Zhou, J.-H. Wang, J.-R. Yang, D. Li, *Chem. Commun.* **2011**, *47*, 12441; d) S.-Z. Zhan, M. Li, D. Li, *Chem. Eur. J.* **2013**, *19*, 10217.

[12] a) M. A. Omary, A. A. Mohamed, M. A. Rawashdeh-Omary, J. P. Fackler, Jr., *Coord. Chem. Rev.* **2005**, *249*, 1372; b) H. V. R. Dias, H. V. K. Diyabalanage, M. G. Eldabaja, O. Elbjeirami, M. A. Rawashdeh-Omary, M. A. Omary, *J. Am. Chem. Soc.* **2005**, *127*, 7489; c) M. A. Omary, M. A. Rawashdeh-Omary, M. W. A. Gonser, O. Elbjeirami, T. Grimes, T. R. Cundari, *Inorg. Chem.* **2005**, *44*, 8200; d) S. M. Tekarli, T. R. Cundari, M. A. Omary, *J. Am. Chem. Soc.* **2008**, *130*, 1669; e) A. C. Jahnke, K. Pröpper, C. Bronner, J. Teichgräber, S. Dechert, M. John, O. S. Wenger, F. Meyer, *J. Am. Chem. Soc.* **2012**, *134*, 2938.

[13] a) H. Schmidbaur, A. Schier, *Chem. Soc. Rev.* **2008**, *37*, 1931; b) H. Schmidbaur, A. Schier, *Chem. Soc. Rev.* **2012**, *41*, 370.

[14] a) A. Kishimura, T. Yamashita, T. Aida, *J. Am. Chem. Soc.* **2005**, *127*, 179; b) H. O. Lintang, K. Kinbara, K. Tanaka, T. Yamashita, T. Aida, *Angew. Chem.* **2010**, *122*, 4337; *Angew. Chem. Int. Ed.* **2010**, *49*, 4241; c) H. O. Lintang, K. Kinbara, T. Yamashita, T. Aida, *Chem. Asian J.* **2012**, *7*, 2068.
[15] a) B. Willy, T. J. J. Müller, *Eur. J. Org. Chem.* **2008**, 4157; b) P. C. Andrews, G. B. Deacon, W. J. Gee, P. C. Junk, A. Urbatsch, *Eur. J. Inorg. Chem.* **2012**, 3273.
[16] a) G. Yang, R. G. Raptis, *Inorg. Chem.* **2003**, *42*, 261; b) C. Yang, M. Messerschmidt, P. Coppens, M. A. Omary, *Inorg. Chem.* **2006**, *45*, 6592; c) T. Osuga, T. Murase, K. Ono, Y. Yamauchi, M. Fujita, *J. Am. Chem. Soc.* **2010**, *132*, 15553; d) J. Liang, Z. Chen, J. Yin, G.-A. Yu, S. H. Liu, *Chem. Commun.* **2013**, *49*, 3567.
[17] a) I. I. Vorontsov, A. Y. Kovalevsky, Y.-S. Chen, T. Graber, M. Gembicky, I. V. Novozhilova, M. A. Omary, P. Coppens, *Phys. Rev. Lett.* **2005**, *94*, 193003; b) T. Grimes, M. A. Omary, H. V. R. Dias, T. R. Cundari, *J. Phys. Chem. A* **2006**, *110*, 5823; c) B. Hu, G. Gahungu, J. Zhang, *J. Phys. Chem. A* **2007**, *111*, 4965.
[18] CCDC 942719, 942720, 961201 and 961202 contain the supplementary crystallographic data for this paper. These data can be obtained free of charge from The Cambridge Crystallographic Data Centre via www.ccdc.cam.ac.uk/data_request/cif).

